

## Characterisation and Numerical Modelling of the Geometry of Rock Joints

Ricardo P. Resende<sup>a\*</sup>, Ana L. Ramos<sup>b</sup>, José R. Muralha<sup>c</sup>, Eduardo C. Fortunato<sup>c</sup>, Luís N. Lamas<sup>c</sup>

<sup>a</sup> *University Institute of Lisboa (ISCTE-IUL), ISTAR, Lisbon, Portugal*  
<sup>b</sup> *Faculty of Engineering of the Porto University (FEUP), Porto, Portugal*  
<sup>c</sup> *National Laboratory for Civil Engineering (LNEC), Lisbon, Portugal*  
 \* jrpre@iscte.pt

### Abstract

This paper describes the measurement and analysis of the roughness of natural rock joints with the aim of proceeding to their characterisation and comparison. Eight rock joints (corresponding to sixteen surfaces) were scanned with a three-dimensional scanner. This was followed by the description and characterisation of the surface roughness, as well as its reproduction and generation using techniques such as fractal models and Fourier transforms. Shear tests under constant normal load were performed, the joint surfaces were again scanned, and the resulting roughness surfaces were compared allowing the evaluation of asperity breakage and surface wear. One of the joint specimens was tested under several normal stresses, which allowed the estimation of its mechanical characteristics, and was scanned after each test to evaluate the influence of the normal and shear load on the variation of roughness.

The scans of the rock joints produced accurate numerical descriptions of their topologies, allowing countless possibilities of future studies, such as the study of the matching of rock joints by the numerical adjustment of bottom and top surfaces, the statistical and geostatistical characterisation of rock joints or the degradation of roughness after normal and shear tests. This paper presents an overview of the research work that is still under way.

**Keywords:** rock joints, roughness characterisation parameters, surface wear, shear tests

### 1. Introduction

Mechanical and hydraulic behaviour of rock masses is heavily dependent on the existing discontinuities, whether they are faults or joints, schistosity or foliation surfaces (Priest, 1993). The study of the shear strength, deformability and conductivity of rock discontinuities implies the analysis of several factors: roughness and hardness of the joint walls, surface friction and weathering, presence and strength of filling materials and gouge and fluid pressure. In the case of rock joints, the roughness has a large influence on the shear strength, both peak and residual stress. Shear displacement occurs simultaneously with normal displacement (dilatancy) and with shearing of asperities that constitute the roughness, depending on the relationship between the normal stress and the strength of the asperities.

Typically, for a rock joint under constant normal stress and increasing shear loading, the shear displacement begins to increase at a relatively low and approximately constant rate (the shear stiffness) until it reaches a maximum value, the peak shear stress, from which the tangential displacement increases without significant variation of shear stress (Wittke, 1990). It is possible to find in the literature various models for the shear strength. Among the most generally accepted and implemented are:

- the Coulomb model, associated to planar or slightly rough joints;
- the Patton model (1966), which considers a bilinear behaviour, which includes a geometric roughness parameters at low normal stresses;

$$\tau_p = \sigma_n \tan(\phi + i) \quad (1)$$

- and the Barton model (1973), who was the first investigator to explicitly introduce a roughness parameters in the determination of the peak shear strength:

$$\tau_p = \sigma_n \tan \left( JRC \log_{10} \frac{JCS}{\sigma_n} + \phi_r \right) \quad (2)$$

where  $\tau_p$  is the tangential peak strength,  $\sigma_n$  is the normal stress,  $\phi$  is the friction angle,  $i$  is the dilation angle,  $JRC$  (Joint Roughness Coefficient) is the parameter that quantifies the roughness of the surfaces,  $JCS$  (Joint Compressive Strength) is the parameter that evaluates the strength of the rock in the joint surfaces, and  $\phi_r$  is the residual friction angle. This latter parameter depends on the compressive strength of the rock and its weathering state. The determination of the  $JRC$  parameter may be quite subjective, as it can be determined by visual comparison between the joint surface and typical profiles (Barton and Choubey, 1977), though it should preferably be determined by laboratory tilt or pull tests, according to its authors.

## 2. Roughness measurement

Rock joint surface roughness is a characteristic of difficult quantification and the methods employed for its measuring have marked impact on the quality of the results. Currently there are methods that provide data in two dimensions (profiles) and in three dimensions (grid surfaces). Methods can be classified as contact-based, such as mechanical contact profilometers with roller-tip or with a needle-tip, and non-contact, such as laser profilometers, which use the reflection of concentrated light beams, or interferometry-based, where single or multiple cameras detect the geometry of the surface which is lit by a determined light pattern. All these systems have advantages and disadvantages, related to ease and speed of measurement, accuracy, sample size, repeatability, spatial resolution, interface with data analysis methods and in situ usability (Grasselli, 2001).

In this work, a Roland MDX-20 scanner was used (Figure 1). It is a 3D needle-tip contact scanner, which allows the three-dimensional scan of solids with a resolution of 0.05 mm over the horizontal plane ( $x$  and  $y$  directions) and of 0.025 mm in the vertical plane ( $z$  direction). The 0.08 mm diameter needle is a high-precision tool connected to a piezo-electric sensor able to scan objects with maximum size  $203.2 \times 152.4 \text{ mm}^2$  and a maximum height of 60.3 mm above the scanning table. These dimensions limit the size of the rock joints that can be scanned. However, most rock mechanics shear testing apparatuses, including the one that was used, are able to hold rock joint samples up to  $200 \times 150 \text{ mm}^2$ .

After some preliminary tests, a horizontal resolution of 0.5 mm was adopted, which allows scanning the surface of a rock joint sample in six to ten hours. The detail level was judged appropriate taking into account that the grain size in the granite samples under study is approximately 2 mm. The initial tests showed that a higher resolution would not significantly improve data quality, while increasing significantly data acquisition duration and encumbering the data handling and processing. A dedicated software (*Dr.Picza*) from the scanner manufacturer controls the scanning process, checks its quality, allows for a rough visualisation of the scanned surface and exports the data in a variety of formats. Posterior processing and analysis was performed with specific routines developed in *Matlab*.



Fig. 1. The scanner with a joint specimen positioned with the Perspex frame, the surface of a rock joint and its corresponding digital image rendered by the scanner control software.

Specimens analysed in this work were collected within the framework of the study of geological-geotechnical characterisation for the Foz Tua hydroelectric power scheme (Ramos, 2013). The rock joints were sampled from cores collected in boreholes, around 120 mm in diameter, drilled to perform overcoring (STT) tests at depths from 60 to 80 meters. The rock is a medium grain-sized granite with two micas and feldspar phenocrystals of yellowish to greyish colour. The joints present

inclinations of 30°, 45° and 70° with the borehole axis, and some have reddish oxide deposition and a thin film of iron oxide and thin white clay. During the survey, collection, coring, cutting and encasing of the discontinuities, great care was taken in order to minimize the damage to the joint surfaces. Figure 2 presents some of the steps of the preparation of eight joint specimens for the scanning of the surfaces and shear testing.



Fig. 2. Specimen preparation: rock core with joint (left); trimmed rock joints (centre); samples being encased in concrete (right).

After the first scans, it was concluded that to ensure the repeatability of the procedure, it was necessary to devise a technique to ensure the exact placement of the specimens in successive scans. Repeatability is particularly relevant in this study, since roughness measurements are going to be performed before and after the shear tests to assess surface wear. To achieve this objective, an L-shaped perspex frame was built and tightly fixed to the scanning table, allowing the same placement of the joint specimen.

Repeatability was tested by performing repeated scans of the same joint surface with and without the perspex frame and comparing the corresponding results. Figure 3 shows the results of these consecutive scans for the same given profile (longitudinal or  $x$  direction) without and with frame, and the respective differences. The same analysis was performed for a profile in the transversal direction. The average quadratic errors  $errz$  of the two consecutive readings of these roughness profiles were calculated (Table 1). It can be concluded that error values with the frame dropped more than a tenfold, confirming its efficiency.

Figure 4 exemplifies the result of the scanning and processing of a rock joint surface.

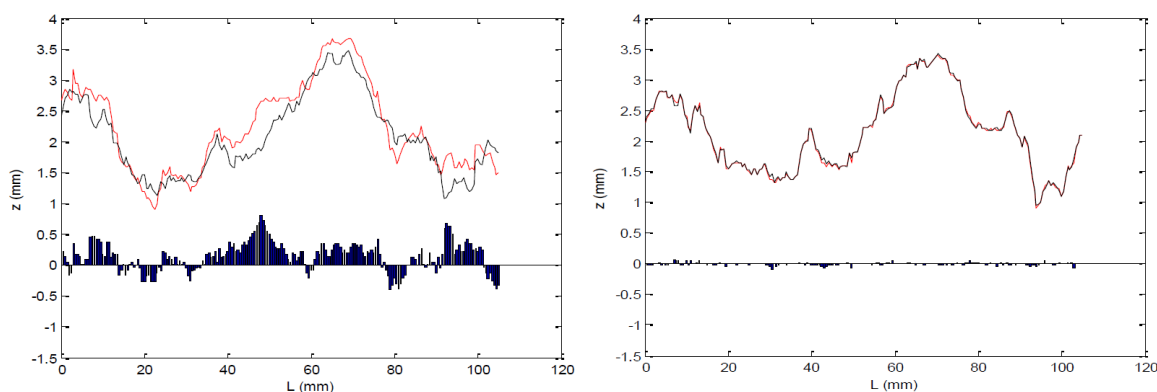


Fig. 3. Two consecutive scans of the same profile (in the  $x$  direction) and respective differences: specimen placed without the frame (left) and using the frame (right).

Table 1. Quadratic error  $errz$  (in  $\text{mm}^2$ ) with and without frame.

	$x$ direction	$y$ direction
Without frame	$7.6 \times 10^{-2}$	$3.6 \times 10^{-3}$
With frame	$5.8 \times 10^{-4}$	$4.2 \times 10^{-6}$

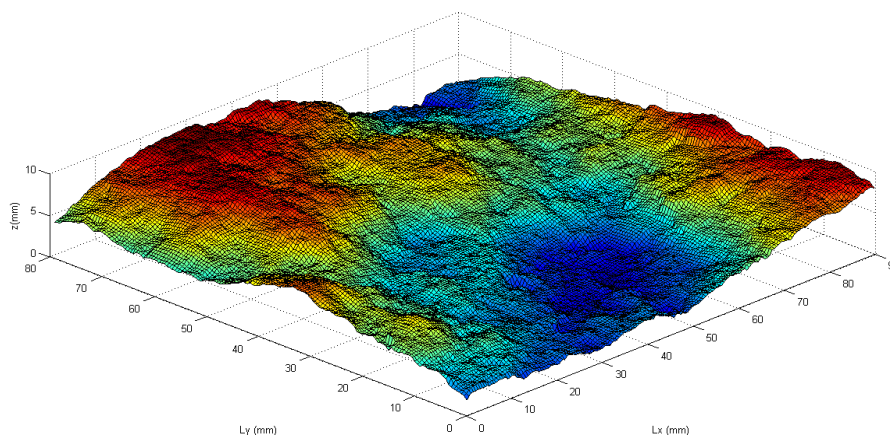


Fig. 4. Example of a rock joint surface.

### 3. Roughness characterisation

Joint roughness characterisation is often based on qualitative approaches, such as the widespread and already mentioned *JRC*. However, several other methodologies have been developed or adapted from other fields of study to quantitatively characterise roughness (Belem *et al*, 2000; Grasselli, 2001). They can be sorted into several categories: statistical, geostatistical, fractal, and Fourier transforms. Generally, they are used to characterise roughness along one dimensional profiles. In this work, 2D analyses were performed extending the methodologies to the whole joint surface. However, since joint shear is intrinsically a directional event, the parameters were calculated along the longitudinal *x* direction of the joints, which is also the direction of the shear tests.

Considering that  $z_{ij}$  is the roughness “height” at a point of a  $n \times m$  grid on the joint, the following formulae were used to evaluate the 2D roughness parameters in this research:

*RMS* – root mean square

$$RMS \cong \sqrt{\frac{1}{nm} \sum_{j=1}^m \sum_{i=1}^{n-1} z_{i,j}^2} \quad (3)$$

*CLA* – central line average

$$CLA \cong \frac{1}{nm} \sum_{j=1}^m \sum_{i=1}^n |z_{ij}| \quad (4)$$

*a* – (maximum) amplitude

$$a \cong \max \{z_{i,j}\} - \min \{z_{i,j}\} \quad (5)$$

*Z<sub>2</sub>* – root mean square of the slopes

$$Z_2 \cong \sqrt{\frac{1}{(n-1)m} \sum_{j=1}^m \sum_{i=1}^{n-1} \left( \frac{z_{i+1,j} - z_{i,j}}{\Delta x} \right)^2} \quad (6)$$

*ACF* – autocorrelation function

$$ACF(k) = \frac{ACV(k)}{ACV(0)} \cong \frac{\frac{1}{m(n-k)} \sum_{j=1}^m \sum_{i=1}^{n-k} z_{i,j} z_{i+k,j}}{\frac{1}{mn} \sum_{j=1}^m \sum_{i=1}^n z_{i,j}^2} \quad (7)$$

$SF$  – structure function

$$SF(k) \cong \frac{1}{m(n-k)} \sum_{j=1}^m \sum_{i=1}^{n-k} (z_{i,j} - z_{i+k,j})^2 = 2RMS^2(1 - ACF(k)) \quad (8)$$

$\gamma(h)$  – semivariogram

$$\gamma(h) \cong \frac{1}{2(n-k)} \sum_{i=1}^{n-k} (z_{i+k} - z_i)^2 \quad (9)$$

In the previous formulae the  $\cong$  symbols intend to establish a distinction between the discrete sampling of the roughness that the scanning yields and the correct mathematical formulation that considers integrals over the joint surface area in place of the sums over the grid points. Since it is likely that the roughness height of a given point is not independent of the heights of its neighbours, formulae (6) to (9) refer to parameters that take this correlation into account. In particular, geostatistics uses the variogram (Matheron, 1965; Chiles and Delfiner, 1999) as an essential tool to assess the dependence and spatial correlation between two neighbouring points. It represents the semivariance of  $z$  between points  $z_i$  and  $z_{i+k}$ , with  $k$  equal to  $h/\Delta x$ , equally spaced at the distance  $h$ . Its value increases with the distance  $h$  until it eventually reaches a constant value as points wide apart do not reveal any correlation.

The concept of fractal (Mandelbrot 1977) is associated with an object with an irregular appearance and whose irregularity is constant irrespective of the scale that is being analysed. This leads to the possibility of the existence of objects with non-integer topological dimensions. In the case of rock joint roughness, the irregularity of the surface of the joint is more complex than a flat surface, but it does not entirely fill a volume; so, its dimension must be between two and three. Consequently, a profile defined along the joint surface must have a fractal dimension higher than one and smaller than two. There are several methods for the estimation of the fractal dimension of a surface or roughness profile, namely, divider, boxes, or balls methods, the Triangular Prisms method, spectral analysis or using the variogram. In this paper, two methods were used to determine the fractal dimension of the rock surfaces: the Revised Triangular Prism Method (RTPM) (de Santis *et al.*, 1997), and the variogram.

RTPM is the extension of Mandelbrot's original dividers method from profiles (1D) to surfaces (2D). The fractal dimension  $D_A$  is determined from the variation of the surface area over various discretizations. For a given discretization  $\Delta x = \Delta y$ , the area is evaluated as the sum of a series of prisms that cover the surface averaging the height  $z$  of the surface at the vertices of each grid element.

The fractal dimension was also determined from the evaluation of the variogram using only the values of two smaller grid resolutions available (0.5 and 1.0 mm). Accordingly, this parameter is referred to as  $D_{V2}$ . This method is similar, in a way, to Mandelbrot's (1977) which determines the fractal dimension of a joint surface by adding 1 to the fractal dimension of a given profile, thus obtaining a fractal dimension between two and three for the surface. However, this latter method is not entirely accurate because the surface fractal dimension is not independent of the chosen profile, or of its direction. Therefore, issues like anisotropy and heterogeneity are ignored (Aydan *et al.*, 1992). To consider the whole surface,  $D_{V2}$  is calculated by averaging the results from all longitudinal profiles of the joint surface.

Figure 4 displays the relation obtained for all 16 (8 joint specimens  $\times$  (top + bottom)). It was found that estimation through the RTPM method led to higher  $D$  values and a larger dispersion in the tested set of joint surfaces.

The surface roughness coefficient  $R_A$  is the ratio between the actual area of the joint surface area and its nominal area (projection of the joint surface on a horizontal plane). Large  $R_A$  values are, thus, associated with rougher surfaces, and inversely, small  $R_A$  values correspond to smoother joints; in the lower bound, an  $R_A$  value of 1 denotes a totally planar joint. The joint surface area can be determined using an algorithm similar to the one used to determine the fractal dimension (RTPM).  $R_A$  values for all eight joints ranged from 1.035 to 1.077, and did not show any correlation with the respective fractal dimensions.

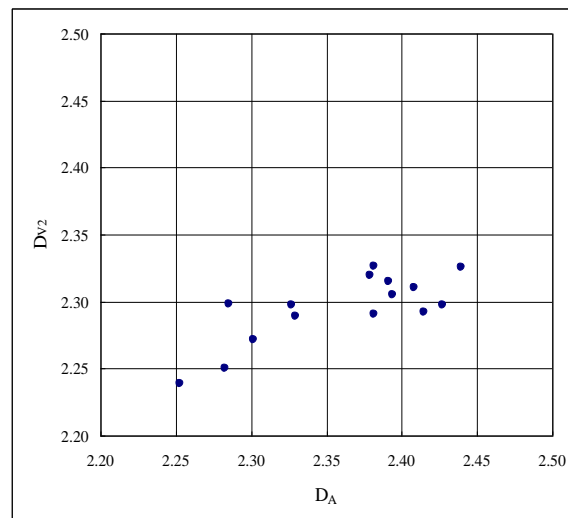


Fig. 4. Relations of the fractal dimensions of all joint surfaces determined by the RTPM  $D_A$  and the variogram methods  $D_{V2}$ .

Figure 5 displays the relative frequency histograms of the distances between the surface scanned heights and the surface mean height for the top and bottom surfaces of specimens 69 and 71. These specimens display the smallest and largest amplitudes, respectively. These graphs show that specimen 69 is rougher than specimen 71, and it also displays a smaller difference between the top and bottom histograms, leading to expect that joint surface matching will be better in specimen 69 than in specimen 71.

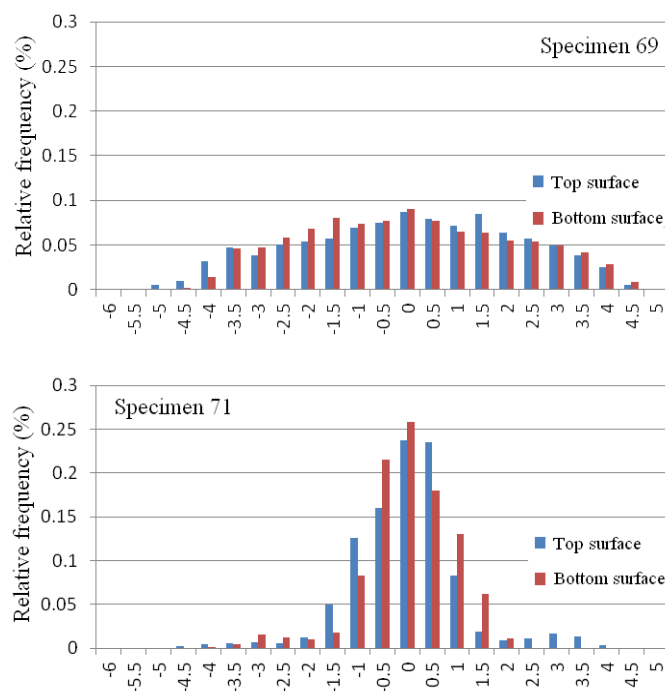


Fig. 5. Frequency histograms of joint heights relative to the average surface height

Correlation between the heights of points along a profile (correlogram) provides information on whether it is possible to estimate the height of a given point from the heights of his neighbouring points. It should be noted that the correlogram is also calculated in a given direction; in this case, it was again taken in the direction of shear. Through the correlogram it is also possible to find the distance upon which there is no relationship between the surface heights. Correlograms for distances between points of 0.5, 1.0, 2.5 and 5.0 mm were calculated, and Figure 6 displays the results obtained for all profiles of the bottom surface of specimen 71. The figure shows that dispersion increases with the lag distance.

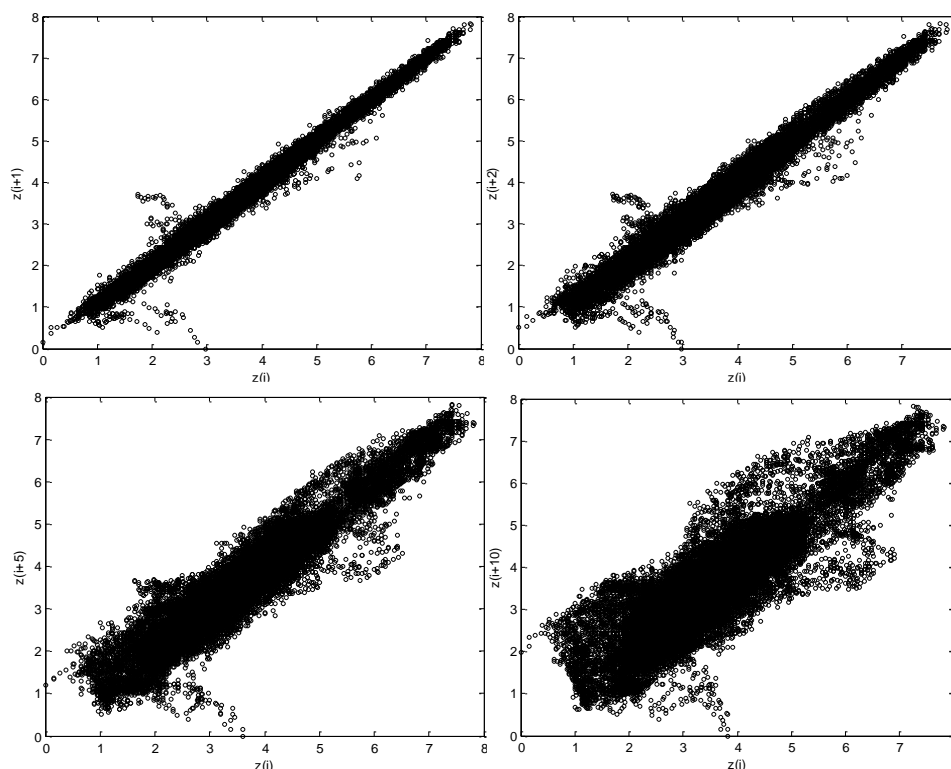


Fig. 6. Surface correlograms for distances (*lag*) of 0.5 ( $i+1$ ), 1.0 ( $i+2$ ), 2.5 ( $i+5$ ) and 5.0 mm ( $i+10$ )

The autocorrelation function *ACF* corresponds to a normalized autocovariance function and discloses the self-dependency of the heights with distance, in a defined direction (the direction of shear tests, in this work). Autocorrelation functions are reasonably similar for all specimens (Figure 7, left), and thus constitute an average parameter for this set of roughness surfaces. In this work the distance, or lag, at which the correlation is equal to 95, 90, 85 and 0% was calculated and the following values were obtained: 0.84 to 1.61 for 95%, 1.48 to 3.09 mm for 90%, 2.13 to 4.04 mm for 85% and 25.19 to 15.19 mm for 0%. These last values mean that heights of points 15 to 25 mm apart do not correlate at all.

Semivariograms of all surfaces were also calculated. The top and bottom of each joint sample is relatively similar (Figure 7, right), as it could be expected. However, there are significant differences between the different samples, unlike what occurred with the autocorrelation function. The semivariograms show some scattering for distances close to 60 mm and some specimens display a small plateau.

Comparing the different correlation techniques (Figure 8), it can be concluded that the values determined for the correlation thresholds are quite different themselves, with the semivariogram values being always significantly higher.

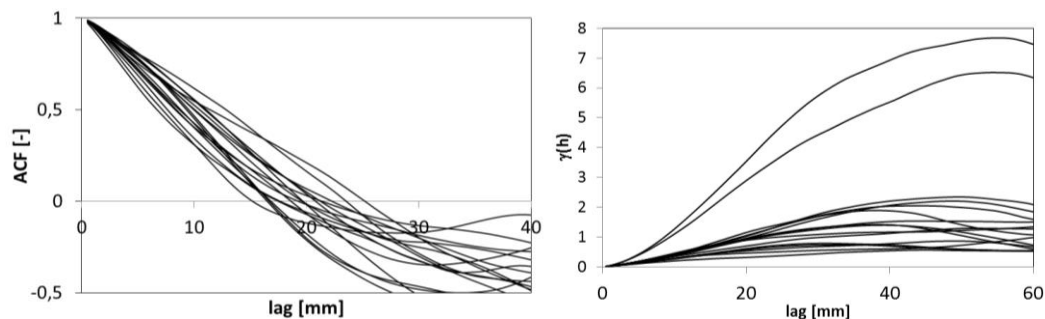


Fig. 7. Roughness analysis: *ACF* autocorrelation functions (left) and semivariograms (right).

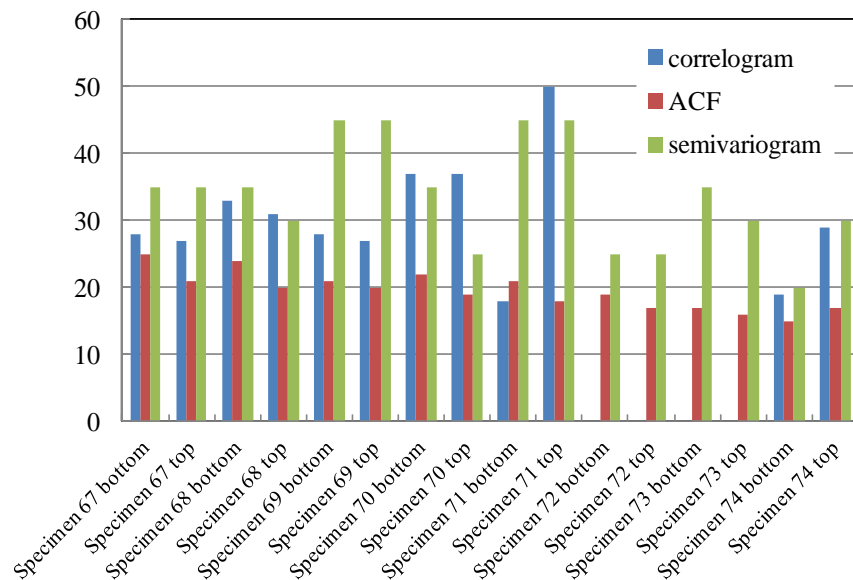


Fig. 8. Comparison of correlation threshold values determined by the three methods.

#### 4. Shear tests

For the characterisation of resistance and deformability of the rock joints, normal and shear loading tests were performed at LNEC Rock Mechanics Laboratory, following the ISRM Suggested Method (Muralha *et al*, 2014). The normal load tests were done prior to the shear tests and consisted on three loading-unloading closure cycles. The closure tests were followed by shear tests under constant normal loading conditions. The equipment consists of a rigid frame that holds to hydraulic jacks that load a  $200 \times 200 \text{ mm}^2$  shear box where the bottom half of the joint specimen is fastened.

Shear tests with a normal stress of 0.4 MPa conducted on the eight specimens allowed to determine the shear stiffness values, which ranged between 0.7 and 1.7 MPa/mm (average of 1.0 MPa/mm), and the peak shear stresses around 0.3 - 0.4 MPa (average 0.37 MPa). Specimen 71 was further subjected to four successive shear tests (Figure 9) with higher normal stresses: 0.4, 0.8, 1.6, and 3.2 MPa. With these four tests it was possible to calculate the Coulomb model parameters for this sample: friction angle of  $35.6^\circ$ , apparent cohesion of 0.11 MPa and dilation angle around  $7.5^\circ$ .

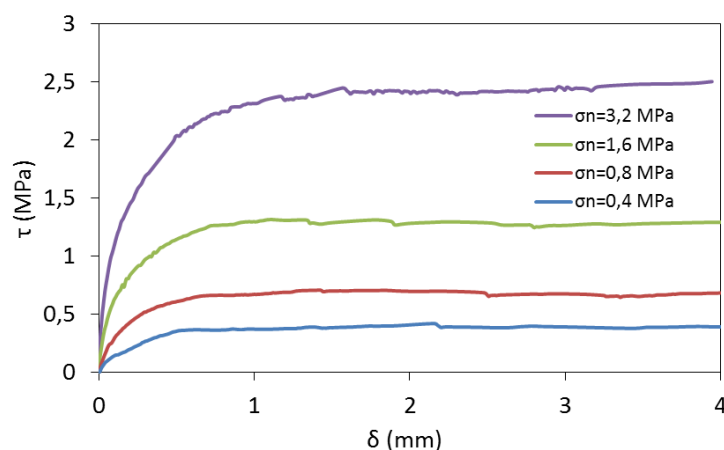


Fig. 9. Shear stress versus shear displacement graphs for specimen 71 b).

Joint walls wear during sliding and therefore a decrease of roughness is expected. Since the samples were scanned before and after the shear tests, the roughness wear can be measured and quantified. However, the comparison of the roughness parameters prior to the tests and after them did not show relevant differences.



The geostatistical analysis does show some differences, though, in some specimens, the variation is not significant. In what regards the fractal dimension, considering both the method of the areas and the semivariogram, the average reduction was 0.7% and 0.6%, respectively. The parameter  $R_A$  had also a very small decrease, 0.8% on average, and  $Z_2$  declined, also on average, 2.8%. These comparisons allow concluding that the shear tests under the normal stress of 0.4 MPa caused little wear to the joint surfaces. Visually, the differences are almost unnoticeable.

In the case of specimen 71, the shear tests were performed repeatedly under higher normal stresses (up to 3.2 MPa). However, since this joint sample showed relatively little initial roughness, the decrease in the parameters was also quite small.

Figure 10 shows equal height plots of the joint specimen 71 before and after the shear the shear test under the lowest normal stress (0.4 MPa). The difference between both scans is also displayed, showing that the wear is concentrated in a very small area.

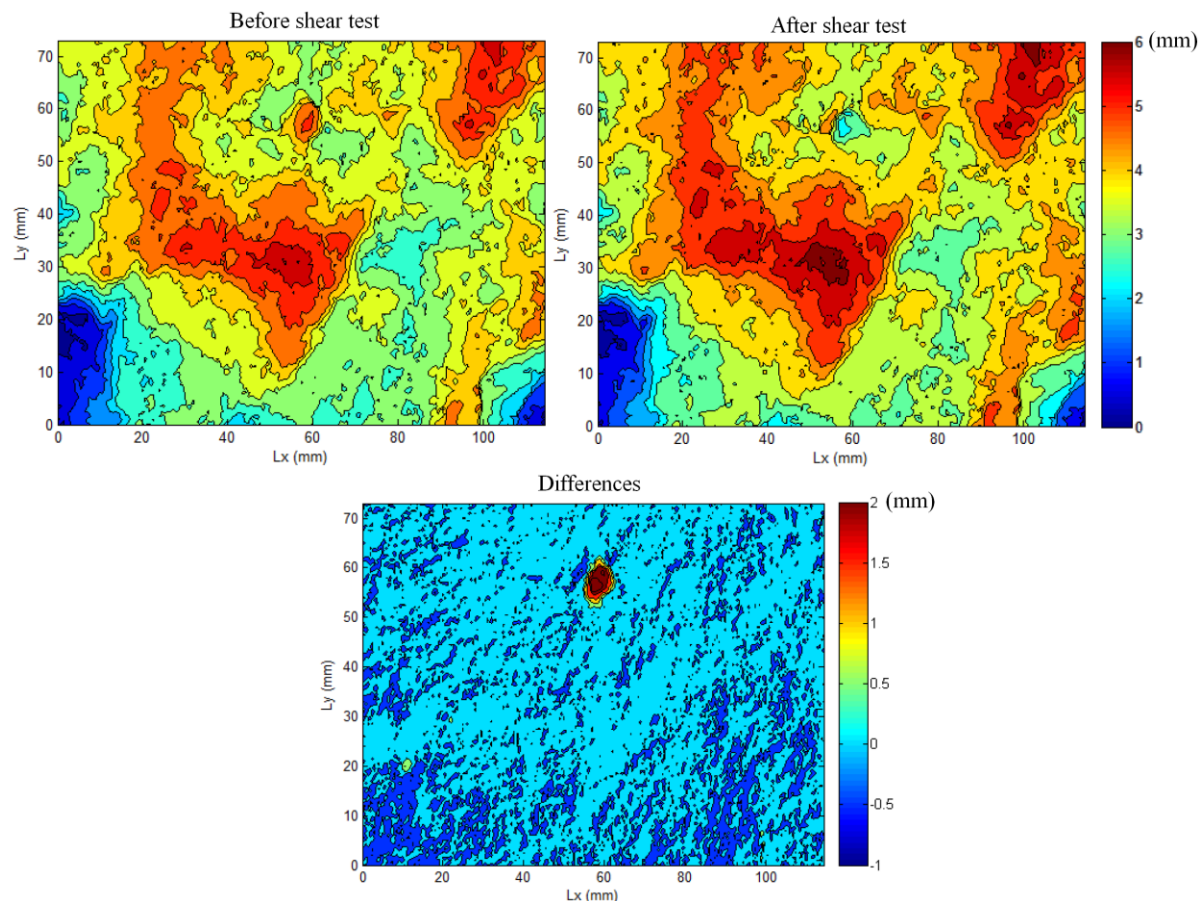


Fig. 10. Iso-heights plot of joint specimen 71 before (upper left) and after the shear test under 0.4 MPa (upper right) and differences between both surfaces (below).

## 5. Conclusions

Joint roughness, along with the strength of the walls, controls the mechanical, hydraulic and dynamic behaviour of rock discontinuities. Roughness is, however, one of the most difficult properties to characterise, for its variability and, complexity as well as by the difficulty in simply measuring it. This paper presents a methodology for measuring joint surfaces, which was made repeatable, robust and with a suitable level of precision and spatial resolution, as well as keeping the measuring procedure within a reasonable duration. It allows not only a deeper and more detailed understanding of the behaviour of these surfaces at a scale that is rarely studied, but also opens the path for rock discontinuity modelling at a micromechanical level, such as the discrete elements or particles method.

The scans of the rock joints produced accurate numerical descriptions of their topologies, opening many possibilities, such as the study of the matching of rock joints by numerical adjustment of bottom and top surfaces, the statistical and geostatistical characterisation of rock joint roughness degradation after normal and shear tests, or the study of the voids network in a fracture. This paper presents an

overview of the research work that is still under way. The generation of new artificial surfaces from existing surfaces using two-dimensional Fourier analysis and the fractal dimension is another topic that has already been accomplished, but was not included in this paper due to lack of space.

Various statistical and geostatistical parameters of the joint surfaces, such as the variogram, fractal dimension or the surface roughness coefficient, were calculated and analysed. In relation to the statistical parameters, it was concluded that  $Z_2$ , the mean square of the slope between two consecutive points, as it favours the direction of shear displacement of the shear tests, allows obtaining a value that characterises the roughness and the waviness of the surface. The fractal dimension  $D$ , calculated by several methods that were compared, considers the three-dimensional features of discontinuity and characterises the roughness. Finally, the comparison of the surfaces before and after shear tests, aided by the evolution of the parameters, is expected to help to understand the joint surface wear and degradation. The joint roughness characterisation that was presented is intended to be used as a benchmark for numerical models that aim at reproducing the complex dynamic, hydraulic and mechanical behaviour of joints.

### Acknowledgements

The authors are deeply thankful to EDP (Electricidade de Portugal) for allowing to sample the joints from the cores that were executed during the rock mass geotechnical characterisation performed for the Foz Tua hydroelectric scheme, for enabling to use the FabLab facilities where the equipment that was used to scan the joint surfaces is accessible, and to present the results of this research.

### References

- Aydan, Ö., Shimizu, Y. and Kawamoto, T., 1992, The anisotropy of surface morphology characteristics of rock discontinuities, *Rock Mechanics and Rock Engineering*, 29 (1), 47-59.
- Barton, N., 1973, Review of a new shear strength criterion for rock joints, *Engineering Geology*, 7, 287-332.
- Barton, N. and Choubey, V., 1977, The shear strength of rock joints in theory and practice, *Rock Mechanics*, 10, 1-54.
- Barton, N., 2013, Shear strength criteria for rock, rock joints, rockfill and rock masses: Problems and some solutions, *Journal of Rock Mechanics and Geotechnical Engineering*, 5, 249-261.
- Belem, T., Homand-Etienne, F. and Souley, M., 2000, Quantitative parameters for rock joint surface roughness, *Rock Mechanics and Rock Engineering*, 33(4), 217-242.
- Similar Publications.
- Chilès, J.-P. and Delfiner, P., 1999, *Geostatistics: Modeling spatial uncertainty*, Wiley, New York.
- Grasselli, G., 2001, Shear strength of rock joints based on quantified surface description, PhD thesis, École Polytechnique Fédérale de Lausanne.
- Mandelbrot, B.B., 1977, *The fractal geometry of Nature*, W.H. Freeman, New York.
- Matheron, G., 1965, *Les variables régionalisées et leur estimation*, PhD thesis, Masson, Paris.
- Muralha, J., Grasselli, G., Tatone, B., Blümel, M., Chryssanthakis, P. and Jiang Y., 2014, ISRM Suggested Method for laboratory determination of the shear strength of rock joints: Revised version, *Rock Mechanics and Rock Engineering*, 47, 291-302.
- Patton, F.D., 1966, Multiple modes of shear failure in rock, PhD thesis, Urbana University, Illinois.
- Priest, S.D., 1993, *Discontinuity analysis for rock engineering*, 1<sup>st</sup> ed. Chapman & Hall, London, 473 p.
- Ramos, A.L., 2013, Characterisation and modelling of the roughness of rock discontinuities (in Portuguese), MSc thesis, Faculty of Engineering of the Porto University.
- de Santis, A., Fedi, L. and Quadra, T., 1997, A revisit of the triangular prism surface area method for estimating the fractal dimension of the fractal surfaces, *Annali di Geofisica*, XL(4), 811-821.
- Wittke, W., 1990, *Rock mechanics: Theory and applications with case histories*, Springer-Verlag, Berlin.